Optimal Scalogram for Computational Complexity Reduction in Acoustic Recognition Using Deep Learning

Dang Thoai Phan*, Tuan Anh Huynh†, Van Tuan Pham‡,
Cao Minh Tran§, Van Thuan Mai¶, Ngoc Quy Tran‖

*Software Development Department, Joyson Safety Systems, Berlin, Germany; thoaidang.phan@joysonsafety.com
†Faculty of Software Engineering, University of Information Technology, Ho Chi Minh city, Vietnam
Vietnam National University, Ho Chi Minh city, Vietnam; anhht@uit.edu.vn
‡Artificial Intelligence, Yokogawa Votiva Solutions, Ho Chi Minh city, Vietnam; tuan.pham@votivasoft.com
§Information Technology, Nguyen Tat Thanh University, Ho Chi Minh city, Vietnam; trancaominhkg@gmail.com
¶Smart Ocean Mobility, Changwon National University, Changwon, Republic of Korea; maivanthuan996@gmail.com
‖Software Engineering, FPT University Hanoi, Hanoi, Vietnam; quytnhe161643@fpt.edu.vn

Abstract—The Continuous Wavelet Transform (CWT) is an effective tool for feature extraction in acoustic recognition using Convolutional Neural Networks (CNNs), particularly when applied to non-stationary audio. However, its high computational cost poses a significant challenge, often leading researchers to prefer alternative methods such as the Short-Time Fourier Transform (STFT). To address this issue, this paper proposes a method to reduce the computational complexity of CWT by optimizing the length of the wavelet kernel and the hop size of the output scalogram. Experimental results demonstrate that the proposed approach significantly reduces computational cost while maintaining the robust performance of the trained model in acoustic recognition tasks.

Index Terms—Continuous Wavelet Transform, Wavelet Kernel Length, Scalogram, Hop Size, Acoustic Recognition.

I. INTRODUCTION

Feature extraction from time-series signals is a critical step in many deep learning applications, particularly when combined with architectures such as Convolutional Neural Networks (CNNs) [1]–[5]. Among the various techniques available, the Continuous Wavelet Transform (CWT) has emerged as a widely adopted method, especially in processing acoustic signals, due to its multiresolution analysis capability [6] that enhances model performance [2], [7]. Significant research efforts have been dedicated to leveraging WT for improved feature representation [8]–[13].

For instance, Copiaco [14] utilized scalograms derived from the CWT as spectro-temporal features for domestic audio classification. These scalograms were input into a hybrid model comprising CNNs and a Support Vector Machine (SVM), resulting in notable performance improvements compared to top-performing baseline models. Similarly, Gupta [15] employed CNNs with CWT-based scalograms for voice liveness detection. Their method effectively differentiated between genuine and spoofed speech using a handcrafted Morlet wavelet—substantially outperforming the Short-Time Fourier Transform (STFT) spectrogram. In another study, Chatterjee
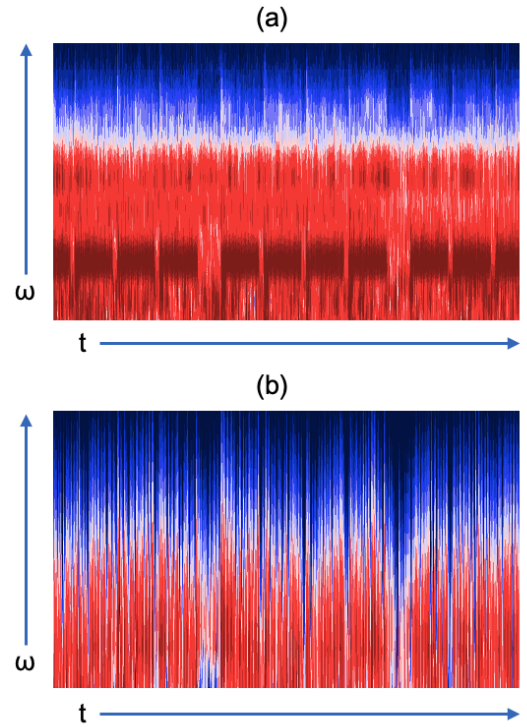

Fig. 1. Scalogram of CWT (a); optCWT (b)

[16] addressed musical instrument identification by transforming audio samples into CWT-based scalograms and utilizing a combination of Convolutional Siamese Networks and Residual Siamese Networks. Their approach attained an impressive classification accuracy using only five training samples per class from public datasets. Phan [2] conducted a comparative analysis of CWT and STFT as inputs to CNN models for non-stationary machine noise classification. While results favored

the CWT in terms of recognition performance, the study also underscored its high computational cost.

These recent contributions highlight the effectiveness of CWT as a time-frequency feature extractor [17]–[27]. Nonetheless, a major limitation lies in its computational burden: CWT must be computed continuously over each sample in a discrete signal, resulting in substantial data volume and potential redundancy due to similarities among adjacent samples. Consequently, alternative methods such as the STFT [1], [28]–[35] are often preferred for their computational efficiency.

Given this context, there is a growing need for approaches that preserve the advantages of CWT's multiresolution analysis while mitigating its computational demands. Developing such techniques could significantly improve the practicality and scalability of CWT-based models in real-world applications.

II. THEORETICAL FOUNDATION

A. Wavelet transform

WT is a technique that decomposes a signal into a form that better represents the original signal's features for further processing [36]. In acoustic recognition, WT converts a one-dimensional (1D) time signal into a two-dimensional (2D) time-frequency plane, as described by the calculation formula in (1). WT is a function of time translation b and frequency shift a. The signal's energy is normalized by the factor $1/\sqrt{a}$ to ensure consistent energy levels across all frequency scales. The wavelet is contracted and dilated according to the varying scale, and each scaled wavelet is then shifted along the time axis to convolve with the signal $x(t)$.

$$X_{WT}(b,a) = \frac{1}{\sqrt{a}} \int_{-\infty}^{\infty} x(t)\psi^*(\frac{t-b}{a})\, dt \qquad (1)$$

The CWT in discrete form is given by:

$$W_{WT}(b,a) = \frac{1}{\sqrt{a}} \sum_{n=0}^{N-1} x[n] \cdot \psi^* \left(\frac{n-b}{a} \right) \qquad (2)$$

where: n is the discrete time index, $x[n]$ is the discrete signal of length N. CWT for a time-discrete signal is computed by the discrete summation of the dot product within the sampling interval. The translation parameter b and scale parameter a are in continuous forms, where translation is sample-wise, and scale spans a range of continuous natural numbers. This process produces a coefficient matrix of size (N, a), where N is the data length and a is the scales range. The scalogram of CWT is illustrated in Fig. 1(a), with the vertical direction representing the frequency/scale (ω/a) and the horizontal direction representing the time/translation (t/b).

The CWT is commonly implemented using the PyWavelets [37] library, specifically through the pywt.cwt function. However, this function does not provide options for adjusting the wavelet kernel length or customizing the scalogram size based on specific requirements. This limitation results in a high computational cost, particularly for tasks that require low temporal resolution. Therefore, an approach that optimizes computational efficiency while preserving essential time-frequency features is highly desirable.

B. Proposed idea

The proposed approach introduces two complementary methods to optimize computational complexity. Firstly, instead of computing CWT using a pre-defined Morlet wavelet kernel, the approach allows for the adjustment of the Morlet wavelet's length. This modification provides flexibility in balancing temporal resolution and computational cost. For applications requiring high temporal resolution, users can increase the wavelet length *(WL)* to capture more detailed temporal features in the signal. Conversely, for applications prioritizing lower computational cost, the wavelet length can be reduced accordingly.

Secondly, rather than producing a full output length equivalent to the input signal for each scale in the CWT, the proposed approach samples the output using a predefined hop size *(H)* in convolution step of each scale. This strategy reduces the number of extracted temporal features while lowering computational complexity during the CWT process. By performing a grid search over the parameters *(WL)* and *(H)*, users can optimize computational cost at satisfactory performance in trained models.

III. EXPERIMENT

A. Dataset

The present study uses the MIMII dataset [38], which comprises acoustic recordings collected from industrial environments. The dataset includes sound data from various types of machinery, specifically fans, pumps, sliders, and valves. For each machine type, the dataset categorizes audio recordings into two classes: normal, representing properly functioning machinery, and abnormal, corresponding to malfunctioning machinery. The primary objective of utilizing this dataset is to develop and train models for the detection of machinery faults based on audio signals. To enhance robustness, the recordings are superimposed with environmental background noise at three distinct levels of signal-to-noise ratio (SNR): -6 dB, 0 dB, and 6 dB. The dataset consists of 54,507 audio files, each with a duration of 10 seconds. All recordings are sampled at 16 kHz, yielding 160,000 samples per audio file.

B. Scalogram generation

The process of scalogram generation is illustrated in Fig. 2, and is herein referred to as optCWT (optimal continuous wavelet transform). Initially, a wavelet kernel of length *WL* is defined at a given scale *S*. By specifying the wavelet length, the transformation can be tailored to balance the trade-off between prediction performance and computational cost. Specifically, longer wavelets may enhance model performance at the expense of increased computational complexity, whereas shorter wavelets may reduce computational demands with potentially lower performance. Subsequently, the discrete audio signal *x(n)* of length *N*, as obtained from the aforementioned dataset, is convolved with the wavelet kernel using the Fast Fourier Transform (FFT), in accordance with the standard wavelet transform procedure. The resulting output is then downsampled by a factor of *H*, rather than retaining its original
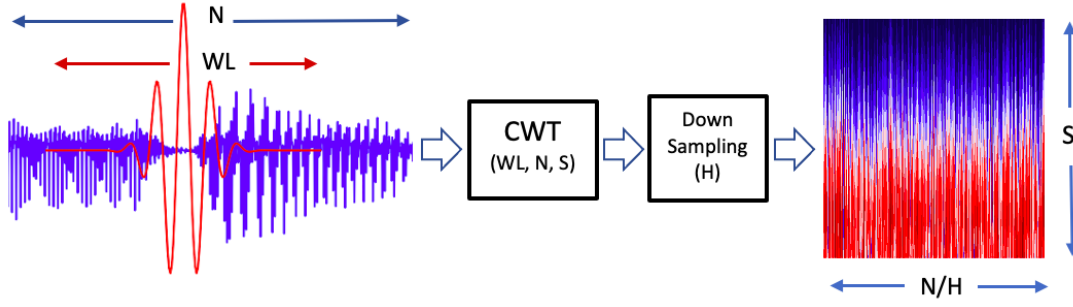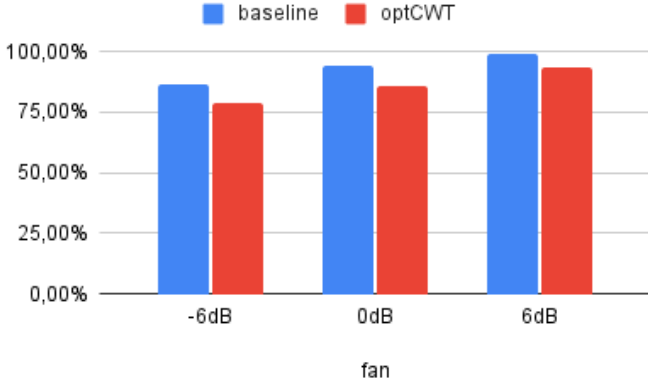
Fig. 2. Scalogram generation

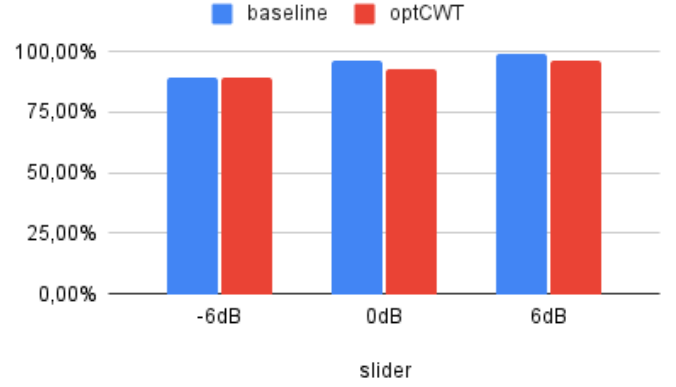Fig. 3. Prediction performance AUC-ROC of models on audio of fan

Fig. 5. Prediction performance of AUC-ROC models on audio of slider
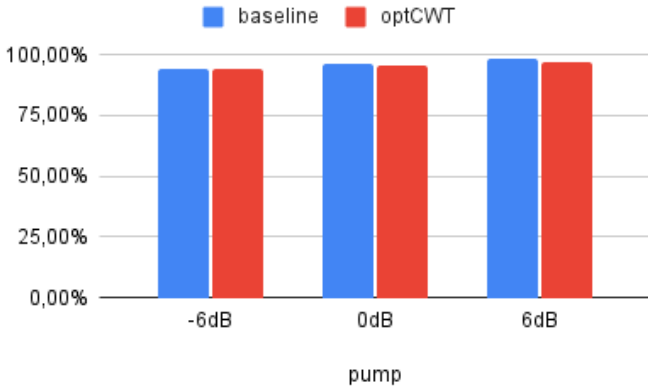

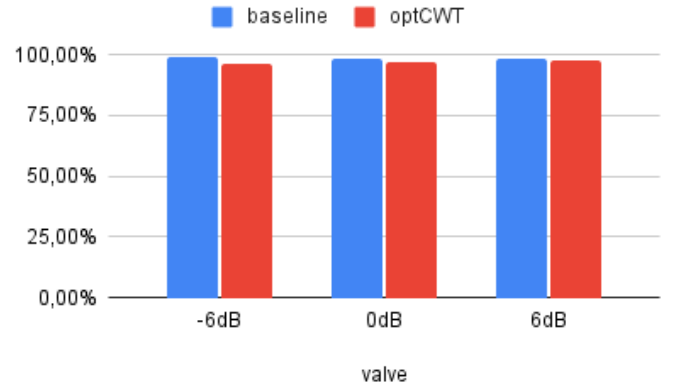Fig. 4. Prediction performance AUC-ROC of models on audio of pump

Fig. 6. Prediction performance AUC-ROC of models on audio of valve

resolution. This downsampling operation reduces both memory usage and computational overhead, thereby optimizing the efficiency of subsequent processing steps, such as heat maps visualization. The transformation is iteratively performed for the same audio signal across the specified range of wavelet scales. Upon completion, a coefficient matrix of dimensions *(N/H, S)* is produced, which is more compact compared to the standard wavelet transform coefficient matrix of size *(N, S)*. This reduced matrix is subsequently utilized to generate

heatmaps, referred to as scalograms. The implementation for scalogram generation in this study has been made publicly available via the GitHub repository referenced in [39], and a pull request proposing the findings to upgrade the Pywavelets library is already created [40]. The configuration of the transform is based on the benchmark study, employing 128 scales of range (2, 129) [2]. For visual comparison, the scalograms produced by both the conventional CWT and the proposed optCWT are presented side by side in Fig. 1 (a) and (b)

TABLE I
PERFORMANCE OF MODELS FOR AUDIO OF FAN

	Baseline	optCWT
-6 dB	86,71%	78,73%
0 dB	94,41%	85,98%
6 dB	99,24%	93,62%

TABLE II
PERFORMANCE OF MODELS FOR AUDIO OF PUMP

	Baseline	optCWT
-6 dB	93,91%	93,96%
0 dB	96,21%	95,34%
6 dB	98,62%	97,13%

TABLE III
PERFORMANCE OF MODELS FOR AUDIO OF SLIDER

	Baseline	optCWT
-6 dB	89,03%	89,40%
0 dB	96,44%	92,67%
6 dB	98,85%	96,24%

TABLE IV
PERFORMANCE OF MODELS FOR AUDIO OF VALVE

	Baseline	optCWT
-6 dB	98,92%	96,64%
0 dB	98,61%	96,87%
6 dB	98,76%	97,54%

respectively. As observed, the CWT-based scalogram exhibits a more continuous and densely concentrated energy distribution, providing a more detailed representation. In contrast, the optCWT scalogram displays a sparser and more discrete distribution of energy, reflecting the trade-offs introduced by the optimized transformation.

C. Acoustic recognition task

To perform the acoustic recognition task, a CNNs model is developed and uses the scalogram images generated in the previous step as input data. The model is trained and tested for performance of fault detection via acoustic recognition. The performance of the optCWT-generated scalograms on the CNNs is evaluated and compared to that of scalograms produced by the conventional CWT to assess the efficacy of optCWT in detecting anomalous sounds. The developed pipeline is identical to the benchmark study [2] for comparison purpose. The settings for scales, heat map generation, and CNN parameters are also adopted from the referenced study. These include an input image size of 512×512 pixels, convolutional layers with a kernel size of 3×3, and a learning rate of 0.001. The model is trained using a batch size of 64 for 32 epochs. The only extra steps are the definition of wavelet kernel length and sampling the output of CWT. Two main parameters of this study, wavelet length *WL* and hop size *H* are examined in grid search manner to find an optimal set *WL = 64, H = 128*, which is significantly reduce the computation cost while achieving a satisfactory performance.

The research employs the PyWavelets library for wavelet transformation, the TensorFlow library for implementing the binary classification CNNs model, and the Area Under the Curve of the Receiver Operating Characteristic (AUC-ROC) [41] as the prediction performance metric.

D. Results

The prediction performance of the models across various audio types is documented in Tables I, II, III and IV, and visualized in Figures 3, 4, 5 and 6. As observed, the predictive performance of both models improves with increasing SNR levels across all four types of machines. This improvement can be attributed to the fact that higher SNR levels yield more distinguishable features, thereby facilitating more effective

training and prediction. In comparing the two models, the baseline model consistently demonstrates performance that is comparable to or superior to that of optCWT, which is likely due to the higher resolution of its wavelet transform.

Notably, the results for the fan and valve machines warrant further discussion. For the fan, both models exhibit lower performance relative to the other machines, with a larger performance gap between the baseline and optCWT. A possible explanation is the stationary nature of fan audio signals [38], which are less effectively represented by wavelet transforms. As a result, the baseline model, which employs a higher-resolution wavelet transform, performs better than optCWT, which utilizes a lower-resolution transform. Conversely, in the case of the valve, which produces non-stationary audio signals [38], both models achieve stable and superior performance across all SNR levels, with a smaller performance gap. This can be attributed to the multi-resolution analysis capability of the wavelet transform, which is particularly effective for extracting features from non-stationary signals. This leads to enhanced performance for both models and reduces the disparity between them. These findings are consistent with the results reported in previous studies [2], [7].

Overall, optCWT delivers performance that is fair and comparable to that of the baseline model, indicating its potential applicability in practical scenarios. Moreover, optCWT offers a substantial computational advantage as recorded in Table V and illustrated in Fig. 7. In the experimental setup, the generation of optCWT for a single file required only 1.15 seconds, whereas the baseline's CWT required 8.09 seconds - approximately seven times longer. For the complete dataset comprising 54,507 files, the total processing time amounted to 17.5 hours for optCWT, compared to 122.5 hours for the baseline CWT. These results underscore the significant computational efficiency of optCWT.

TABLE V
COMPUTATIONAL LOAD FOR A SINGLE FILE

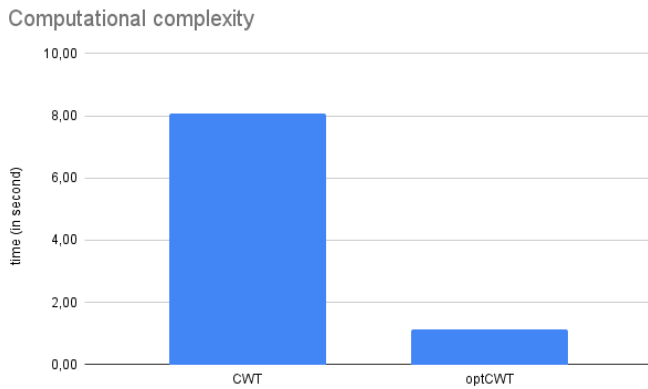| Time	Single audio	Entire dataset
Baseline	8.09s	122.5hrs
optCWT	1.15s	17.5hrs

Fig. 7. Computational complexity in generation of a single file in second

IV. CONCLUSION AND DISCUSSION

This research has developed an efficient method for acoustic recognition by accepting a minor reduction in prediction performance in exchange for a substantial decrease in computational complexity. This trade-off is particularly advantageous for applications requiring real-time processing or operating under limited computational resources.

Future research should explore the use of alternative wavelet types, such as the Mexican Hat wavelet and the Shannon wavelet, to establish a set of wavelets compatible with the proposed method for further reducing computational complexity. Additionally, evaluating the method on diverse datasets is anticipated to enhance the generalizability of its applicability across various types of audio data.

REFERENCES

[1] Z. Jin, L. Lang, and B. Leng, "Wave-spectrogram cross-modal aggregation for audio deepfake detection," in *ICASSP 2025-2025 IEEE International Conference on Acoustics, Speech and Signal Processing (ICASSP)*. IEEE, 2025, pp. 1–5.

[2] D. T. Phan, "Comparison performance of spectrogram and scalogram as input of acoustic recognition task," in *Advances in Information and Communication*, K. Arai, Ed. Cham: Springer Nature Switzerland, 2025, pp. 660–673.

[3] G. Trappolini, A. Purificato, F. Siciliano, L. D'Addona, A. M. Spagnolo, D. Dato, and F. Silvestri, "Quantized auto encoder-based anomaly detection for multivariate time series data in 5g networks," *IEEE Access*, 2025.

[4] K. Cao-Van, T. C. Minh, H. M. Tan *et al.*, "Prediction of heart failure using voting ensemble learning models and novel data normalization techniques," *Engineering Applications of Artificial Intelligence*, vol. 154, p. 110888, 2025.

[5] A. T. Huynh, V.-D. Hoang, S. Vu, T. T. Le, and H. D. Nguyen, "Skin cancer classification using different backbones of convolutional neural networks," in *International Conference on Industrial, Engineering and Other Applications of Applied Intelligent Systems*. Springer, 2022, pp. 160–172.

[6] T. Guo, T. Zhang, E. Lim, M. Lopez-Benitez, F. Ma, and L. Yu, "A review of wavelet analysis and its applications: Challenges and opportunities," *IEEe Access*, vol. 10, pp. 58 869–58 903, 2022.

[7] D. Thoai Phan, "Reduce computational complexity for continuous wavelet transform in acoustic recognition using hop size," in *2024 International Symposium on Electronics and Telecommunications (ISETC)*, 2024, pp. 1–4.

[8] X. Zhao, R. Aridi, J. Hume, S. Subbiah, X. Wu, H. Chung, Y. Qin, and Y. B. Gianchandani, "Automatic peak detection algorithm based on continuous wavelet transform for complex chromatograms from multi-detector micro-scale gas chromatographs," *Journal of Chromatography A*, vol. 1714, p. 464582, 2024. [Online]. Available: https://www.sciencedirect.com/science/article/pii/S0021967323008075

[9] S. M. Shabber, E. Sumesh, and V. L. Ramachandran, "Scalogram based performance comparison of deep learning architectures for dysarthric speech detection," *Artificial Intelligence Review*, vol. 58, no. 5, p. 128, 2025.

[10] P. C. Negi, N. Sharma, S. Sharma *et al.*, "Scalogram sets based motor imagery eeg classification using modified vision transformer: A comparative study on scalogram sets," *Biomedical Signal Processing and Control*, vol. 104, p. 107640, 2025.

[11] H. Yousefpour, S. A. Amiri, and Z. Mohammadpoory, "Bridge anomaly detection via structure health monitoring with resnet-152 and scalogram techniques on vibration data," *Signal, Image and Video Processing*, vol. 19, no. 4, p. 310, 2025.

[12] N. El Assri, M. A. Jallal, S. Chabaa, and A. Zeroual, "Enhancing building energy consumption prediction using lstm, kalman filter, and continuous wavelet transform," *Scientific African*, p. e02560, 2025.

[13] Y.-S. Lee, H.-T. Chung, J.-J. Lin, M.-S. Hwang, H.-C. Liu, H.-M. Hsu, Y.-T. Chang, and S.-J. Peng, "Prediction of significant congenital heart disease in infants and children using continuous wavelet transform and deep convolutional neural network with 12-lead electrocardiogram," *BMC pediatrics*, vol. 25, no. 1, p. 324, 2025.

[14] A. Copiaco, C. Ritz, S. Fasciani, and N. Abdulaziz, "Scalogram neural network activations with machine learning for domestic multi-channel audio classification," in *2019 IEEE International Symposium on Signal Processing and Information Technology (ISSPIT)*. IEEE, 2019, pp. 1–6.

[15] P. Gupta, P. K. Chodingala, and H. A. Patil, "Morlet wavelet-based voice liveness detection using convolutional neural network," in *2022 30th European Signal Processing Conference (EUSIPCO)*. IEEE, 2022, pp. 100–104.

[16] D. Chatterjee, A. Dutta, D. Sil, and A. Chandra, "Deep single shot musical instrument identification using scalograms," in *2023 International Conference on Artificial Intelligence in Information and Communication (ICAIIC)*. IEEE, 2023, pp. 386–389.

[17] S. Rahula and L. Rajanikumari, "Arrhythmia classification using scalogram-based efficientnet," in *2025 IEEE International Students' Conference on Electrical, Electronics and Computer Science (SCEECS)*. IEEE, 2025, pp. 1–5.

[18] M. M. Chanu, K. M. Devi, K. B. Devi, P. C. Irengbam, and S. N. Devi, "Pcg classification using scalogram and cnn classifier," in *Security Issues in Communication Devices, Networks and Computing Models*. CRC Press, 2025, pp. 86–96.

[19] D. Borzelli, M. Morano, S. Fioretti, and F. Di Nardo, "The pooled scalogram: A wavelet-based approach to detect the co-activation of several muscles in the time-frequency domain," *Biomedical Signal Processing and Control*, vol. 99, p. 106802, 2025.

[20] A. Dades and O. Tyr, "Quadratic-phase wavelet scalogram," *Journal of Pseudo-Differential Operators and Applications*, vol. 16, no. 1, p. 17, 2025.

[21] M. Choudhury, M. Tanvir, M. A. Yousuf, N. Islam, and M. Z. Uddin, "Explainable ai-driven scalogram analysis and optimized transfer learning for sleep apnea detection with single-lead electrocardiograms," *Computers in Biology and Medicine*, vol. 187, p. 109769, 2025.

[22] B. Vigneshwaran, R. Manimala, and M. M. Iqbal, "Stacking deep scalogram features with the enhanced gan for defect recognition in power transformers with highly imbalanced partial discharge signals," *IEEE Transactions on Dielectrics and Electrical Insulation*, 2025.

[23] R. B. Ramteke, G. O. Gajbhiye, and V. R. Thool, "Acute mental stress level detection: A ecg-scalogram based attentive convolutional network," *Franklin Open*, p. 100233, 2025.

[24] A. Roozbehi, H. Abbasi, J. O. Davidson, S. K. Dhillon, K. Q. Zhou, G. Wassink, A. J. Gunn, and L. Bennet, "Enhanced eeg seizure recognition after hypoxia-ischemia in fetal sheep using transformer-based wavelet-scalogram deep learning," *Expert Systems with Applications*, vol. 261, p. 125081, 2025.

[25] K. Pal, K. Namrata, A. K. Akella, V. Meena, and S. Padmanaban, "Detection of islanding in ac microgrid using random forest and scalogram image based local binary pattern," in *2025 Fourth International Conference on Power, Control and Computing Technologies (ICPC2T)*. IEEE, 2025, pp. 1–6.

[26] Y. A. Altay and A. V. Fedorov, "Cascade lti system for acoustic emission digital signal processing: Result visualization via scalogram for defect pattern representation," in *2025 27th International Conference on Digital Signal Processing and its Applications (DSPA)*. IEEE, 2025, pp. 1–4.

[27] M. Mostafavi, S.-B. Ko, S. B. Shokouhi, and A. Ayatollahi, "Correction to: Transfer learning and self-distillation for automated detection of schizophrenia using single-channel eeg and scalogram images," *Physical and Engineering Sciences in Medicine*, pp. 1–2, 2025.

[28] D. Kong, H. Yu, and G. Yuan, "Multi-spectral and multi-temporal features fusion with se network for anomalous sound detection," *IEEE Access*, 2024.

[29] M. Telmem, N. Laaidi, and H. Satori, "The impact of mfcc, spectrogram, and mel-spectrogram on deep learning models for amazigh speech recognition system," *International Journal of Speech Technology*, pp. 1–14, 2025.

[30] B. Ma, L. Chen, X. Sun, X. Yang, and Q. Kong, "Must: Multi-channel ultrasonic spectrogram transformer for microdamage detection in metals," *Mechanical Systems and Signal Processing*, vol. 231, p. 112680, 2025.

[31] T. Liu, M. Wang, B. Yang, H. Liu, and S. Yi, "Esernet: Learning spectrogram structure relationship for effective speech emotion recognition with swin transformer in classroom discourse analysis," *Neurocomputing*, vol. 612, p. 128711, 2025.

[32] N. Banerjee, N. Sethi, and S. Borah, "Deep analysis of mfcc and mel spectrogram features to recognize and classify stuttered speech," *Multimedia Tools and Applications*, pp. 1–20, 2025.

[33] M. Dua, N. Chakravarty, S. G. Priya Reddy, A. Bansal, S. Pawar, and S. Dua, "Melcochleagram-deepcnn: sequentially fused spectrogram and the deepcnn classifiers-based audio spoof detection system," *IETE Journal of Research*, vol. 71, no. 1, pp. 65–70, 2025.

[34] M. S. Mekahlia, M. Fezari, and A. Aliouat, "A comparative analysis of constant-q transform, gammatonegram, and mel-spectrogram techniques for ai-aided cardiac diagnostics," *Medical Engineering & Physics*, p. 104302, 2025.

[35] D. Chen, F. Huang, Z. Song, W. Zhu, Y. Yang, and K. Zeng, "Wavespect: A hybrid approach to synthetic audio detection via waveform and spectrogram analysis," in *ICASSP 2025-2025 IEEE International Conference on Acoustics, Speech and Signal Processing (ICASSP)*. IEEE, 2025, pp. 1–5.

[36] P. S. Addison, *The illustrated wavelet transform handbook: introductory theory and applications in science, engineering, medicine and finance*. CRC press, 2017.

[37] G. Lee, R. Gommers, F. Waselewski, K. Wohlfahrt, and A. O'Leary, "Pywavelets: A python package for wavelet analysis," *Journal of Open Source Software*, vol. 4, no. 36, p. 1237, 2019.

[38] H. Purohit, R. Tanabe, K. Ichige, T. Endo, Y. Nikaido, K. Suefusa, and Y. Kawaguchi, "Mimii dataset: Sound dataset for malfunctioning industrial machine investigation and inspection," *arXiv preprint arXiv:1909.09347*, 2019.

[39] D. T. Phan, "Optimal scalogram for computational complexity reduction in acoustic recognition using deep learning," https://github.com/phandangthoai/Optimal_Scalogram, 2025, accessed: 2025-05-18.

[40] ——, "Enhance cwt by introducing a configurable hop size parameter pr no.804," https://github.com/PyWavelets/pywt/pull/804, 2025, accessed: 2025-05-26.

[41] F. J. Provost, T. Fawcett, R. Kohavi *et al.*, "The case against accuracy estimation for comparing induction algorithms." in *ICML*, vol. 98, 1998, pp. 445–453.